Reachability deficit of variational Grover search

Xiao-Wei Li,[1] Xiao-Ming Zhang,[2,3] Bin Cheng,[2,4] and Man-Hong Yung[1,5,6,*]

[1]*Shenzhen Institute for Quantum Science and Engineering, Southern University of Science and Technology, Shenzhen 518055, China*

[2]*Department of Physics, Southern University of Science and Technology, Shenzhen 518055, China*

[3]*Center on Frontiers of Computing Studies, Peking University, Beijing 100871, China*

[4]*Centre for Quantum Software and Information, Faculty of Engineering and Information Technology, University of Technology Sydney, New South Wales 2007, Australia*

[5]*Guangdong Provincial Key Laboratory of Quantum Science and Engineering, Southern University of Science and Technology, Shenzhen 518055, China*

[6]*Shenzhen Key Laboratory of Quantum Science and Engineering, Southern University of Science and Technology, Shenzhen 518055, China*

(Received 25 September 2023; accepted 21 December 2023; published 9 January 2024)

The quantum approximate optimization algorithm (QAOA) is promising for achieving quantum computational advantage with near-term quantum devices. It was numerically shown that the QAOA cost functions exhibit a phenomenon called reachability deficit (RD), where the success probability cannot reach unity until the circuit depth exceeds a certain critical value. However, an in-depth theoretical understanding of RD remains lacking. Here we focus on a variational variant of Grover search on multiple marked solutions as a prototype for analyzing the RD problem, where we further relax the criterion of reachability by tolerating a certain probability of failure. Specifically, we obtain a general analytical expression relating the critical depth of the quantum circuit to the solution density. In the dilute limit, the critical depth is consistent with the Grover bound, exhibiting a robust quadratic scaling that is insensitive to the failure probability. Moreover, we also find that the projective mixing Hamiltonian performs significantly better than the traditional mixing Hamiltonian in the QAOA, although it is less favorable in terms of physical implementation. However, by taking into account two-body interactions in the mixing Hamiltonian, the performance becomes on par with the projective mixing Hamiltonian at the cost of $O(n^2)$ additional terms. These results represent a simplified but insightful model of the QAOA, fully addressing the dependence of required circuit depth over the ground-state degeneracy.

DOI: 10.1103/PhysRevA.109.012414

I. INTRODUCTION

Variational quantum-classical hybrid algorithms have been attracting increasing attention in the field of quantum computation. In particular, the quantum approximate optimization algorithm (QAOA) is becoming a promising algorithm for near-term quantum devices due to its simplicity and low circuit depth. The QAOA was originally developed for solving combinatorial optimization problems such as max-cut problems [1], the maximum independent set [2], the binary paint shop problem [3], binary linear least squares [4], and Max E3LIN2 [5]. It is also widely used to solve practical problems, including portfolio optimization [6], tail assignment [7], protein folding [8], and wireless scheduling [9]. Moreover, it has also been generalized to other problems besides combinatorial optimization problems, such as Grover search [10,11] and a linear system solver [12].

The original version of the Grover search algorithm achieves a quadratic quantum speedup for the problems of searching for a target item in an unstructured data set [13]. It has been generalized to multitarget cases [14] with a nonzero but sufficiently low failure probability. Subsequently, modified versions achieving unit success probability were also proposed [15–18].

On the other hand, it has been shown that the performance of the QAOA depends on the circuit depth and problem density of a specific problem, which characterizes the difficulty of the problem [19,20]. In Ref. [19] Akshay *et al.* showed that for problems like Boolean satisfiability problems and variational Grover search, there are fundamental limits on the performance. When the circuit depth p is lower than a critical value, the minimum cost function can never be achieved regardless of the optimization process. This phenomenon is called the reachability deficit. Akshay *et al.* found that the critical depth is mostly determined by the problem density, a quantity that measures the difficulty of the problem; for k-SAT, it is defined as the ratio of the problem's constraints to variables.

Specifically, in Ref. [19], a single-target version of the variational search problems was considered as one of the examples to explore the reachability deficit of the QAOA. It was observed that there exists a critical depth p^*. If the QAOA depth of the circuit is lower than p^*, the ground-state energy cannot be reached, which means that the target cannot be perfectly found. It was observed that p^* increases quadratically with the number of variables N, which is consistent with the Grover scaling $O(\sqrt{N})$. However, the value of p^* is just estimated with numerical estimation. The exact value

*yung@sustech.edu.cn

of p^* and the minimal cost function that can be reached are still to be determined. Moreover, the generalized problems in different scenarios such as the multitarget search cases are yet to be explored.

In this study we investigate the reachability deficit problem in variational Grover search, where the cost function is the failure probability of finding the targets. In contrast to the constraint-to-variable ratio, we find that the performance of the variational Grover search is contingent on the solution density, the ratio of marked items number M to total items number N. Interestingly, the optimal search depth p exhibits a monotonic decrease with increasing solution density. To quantitatively assess the problem's difficulty, we propose a measure, termed problem hardness, represented by $\alpha := -\log_2(M/N)$. Consequently, we explore multitarget search scenarios and provide analytical expressions for the minimal cost function $C_p^*(\alpha)$ attainable at a given problem hardness α and QAOA depth p.

In particular, we analytically compute the minimum cost function corresponding to any circuit depth. We present a critical problem hardness $\alpha_c(\varepsilon)$ that delineates the achievement of a given failure probability requirement in a single-layer variational quantum search. Specifically, if the problem hardness falls below this critical value, the failure probability requirement can be met using a single layer of the QAOA. Notably, when the failure probability tolerance is set to zero, we obtain the problem hardness corresponding to perfect search, defined as $\alpha_c = 2$, which aligns with prior research [21]. Moreover, we derive the expression for the critical depth $p_\varepsilon^*(\alpha)$ that satisfies the failure probability requirement $C_p^*(\alpha) \leqslant \varepsilon$ for a given problem hardness α. When the circuit depth is greater than or equal to the critical depth, the search satisfying the failure probability requirement can always be achieved. We conduct numerical simulations to validate our analytical results and the numerical results closely match the analytical predictions.

To further investigate the reachability deficit problem, we employ numerical simulations utilizing lower-order Pauli approximations of the projective operator $(|+\rangle\langle+|)^{\otimes n}$ as the mixing Hamiltonian. Our results demonstrate that a contracted mixing Hamiltonian exacerbates the reachability deficit. Nonetheless, at least within the scope of the problem hardness in simulations, our findings highlight that the critical depth for the first-order approximation, in which the mixing Hamiltonian is set to $\sum_i X_i$, scales as $O(\sqrt{N/M})$. In addition, numerically, the second-order approximation $\sum_i X_i + \sum_{ij} X_i X_j$ asymptotically approaches the performance level of the projective operator with increasing problem hardness. This suggests that employing more localized mixing Hamiltonians as alternatives to projective operators can better accommodate the constraints of the noisy intermediate-scale quantum (NISQ) era.

II. VARIATIONAL GROVER SEARCH AS A QUANTUM APPROXIMATE OPTIMIZATION ALGORITHM

A. Quantum approximate optimization algorithm

In the QAOA approach, there are two Hamiltonians H_C and H_B, corresponding to the cost Hamiltonian and the mixing Hamiltonian (or the driver Hamiltonian), respectively. The cost Hamiltonian is related to the optimization problem, whereas the mixing Hamiltonian is designed to be noncommutative to the cost Hamiltonian. A depth-p QAOA ansatz is generated by alternately applying the unitary operators $V_B(\beta_i) = e^{-i\beta_i H_B}$ and $V_C(\gamma_i) = e^{-i\gamma_i H_C}$ to the initial state $|+\rangle^{\otimes n}$, with a total of $2p$ parameters $(\gamma_1, \beta_1, \ldots, \gamma_p, \beta_p)$. In the beginning, the ansatz state with parameters $\boldsymbol{\gamma} = (\gamma_1, \ldots, \gamma_p)$ and $\boldsymbol{\beta} = (\beta_1, \ldots, \beta_p)$ is prepared in the form

$$|\psi(\boldsymbol{\gamma}, \boldsymbol{\beta})\rangle = \prod_{i=1}^{p} e^{-i\beta_i H_B} e^{-i\gamma_i H_C} |+\rangle^{\otimes n}. \tag{1}$$

After the preparation of an ansatz state, the measurement is performed to obtain the expectation of the cost function

$$C_p(\boldsymbol{\gamma}, \boldsymbol{\beta}) := \langle\psi(\boldsymbol{\gamma}, \boldsymbol{\beta})|H_C|\psi(\boldsymbol{\gamma}, \boldsymbol{\beta})\rangle. \tag{2}$$

Then classical optimization loops are applied to minimize the expectation of the cost function.

B. Variational Grover search

In the Grover search algorithm [13,14,22], we are given an oracle unitary operator $U_{\boldsymbol{w}}$ for the set of targets $\boldsymbol{w} = \{w_1, w_2, \ldots, w_M\}$ such that $U_{\boldsymbol{w}}|x\rangle = |x\rangle$ if $x \notin \boldsymbol{w}$ and $U_{\boldsymbol{w}}|x\rangle = -|x\rangle$ if $x \in \boldsymbol{w}$. The goal is to obtain the target state $\frac{1}{\sqrt{M}}\sum_k |w_k\rangle$. The Grover search algorithm consists of $R = O(\sqrt{N/M})$ repeated applications of the Grover iterate $G := U_s U_{\boldsymbol{w}}$, where $U_s := 2(|+\rangle\langle+|)^{\otimes n} - I$ is the Grover diffusion operator. Here n denotes the number of qubits, $N := 2^n$ represents the total number of items, and I denotes the identity operator. The resulting state after applying R Grover iterates is given by

$$|\psi\rangle = G^R|+\rangle^{\otimes n}, \tag{3}$$

where $n = \log_2 N$ is the number of qubits and $|+\rangle^{\otimes n} := (H|0\rangle)^{\otimes n}$ is the equal superposition state. While this algorithm generally achieves success with a probability close to 1 in most cases, it is important to note that the unit success probability cannot be guaranteed in every specific case.

For this reason, variable phases are introduced into the Grover iterate, which is given by

$$G(\phi, \theta) := U_s(\theta) U_{\boldsymbol{\phi}}(\phi), \tag{4}$$

where $U_s(\theta) := (1 - e^{i\theta})(|+\rangle\langle+|)^{\otimes n} - I$ and $U_{\boldsymbol{w}}(\phi) := (1 - e^{i\phi})\sum_k |w_k\rangle\langle w_k| - I$. Note that $G(\pi, \pi) = G$. There exist various approaches to determine these phase variables, encompassing recursive methods [23], analytical methods [15–18], and variational methods [10,11].

In this paper we use the framework of the variational Grover search proposed in Ref. [11]. We introduce this framework in the following and point out it is a QAOA.

C. Variational Grover search as a QAOA

In the QAOA approach of variational Grover search, the cost Hamiltonian of variational Grover search can be set as

$$H_C := I - \sum_{k=1}^{M} |w_k\rangle\langle w_k|. \tag{5}$$

Subsequently, following the QAOA protocol, we have $V_C(\phi_i) = e^{-i\phi_i H_C} = I - (1 - e^{i\phi_i}) \sum_k |w_k\rangle\langle w_k|$, up to a global phase. Thus, $V_C(\phi_i)$ can be considered as the generalization of $U_{\boldsymbol{w}}$ to allow a phase difference, and $V_C(\pi) = U_{\boldsymbol{w}}$. The mixing Hamiltonian H_B is set as

$$H_B = (|+\rangle\langle+|)^{\otimes n}, \tag{6}$$

which gives $V_B(\theta_i) = e^{i\theta_i H_B} = I - (1 - e^{i\theta_i})(|+\rangle\langle+|)^{\otimes n}$. A variational unitary based on H_C and H_B can be constructed as

$$U_p(\boldsymbol{\theta}, \boldsymbol{\phi}) = \prod_{i=1}^{p} V(\theta_i, \phi_i), \tag{7}$$

where

$$V(\theta_i, \phi_i) := V_B(\theta_i) V_C(\phi_i). \tag{8}$$

With initial state $|+\rangle^{\otimes n}$, we obtain an ansatz for the depth-p QAOA

$$|\psi_p(\boldsymbol{\theta}, \boldsymbol{\phi})\rangle = U_p(\boldsymbol{\theta}, \boldsymbol{\phi})|+\rangle^{\otimes n}. \tag{9}$$

Equation (9) reduces to Grover search algorithm by setting $\phi_1 = \theta_1 = \cdots = \phi_p = \theta_p = \pi$.

Since the goal of Grover search is to approach the target state $\frac{1}{\sqrt{M}} \sum_k |w_k\rangle$, a depth-$p$ variational searching problem is equivalent to minimizing the cost function

$$\begin{aligned} C_p(\boldsymbol{\theta}, \boldsymbol{\phi}) &= \langle \psi_p(\boldsymbol{\theta}, \boldsymbol{\phi}) | H_C | \psi_p(\boldsymbol{\theta}, \boldsymbol{\phi}) \rangle \\ &= 1 - \sum_{k=1}^{M} |\langle \psi_p(\boldsymbol{\theta}, \boldsymbol{\phi}) | w_k \rangle|^2. \end{aligned} \tag{10}$$

It is worth noting that $\Pr(k) := |\langle \psi_p(\boldsymbol{\theta}, \boldsymbol{\phi}) | w_k \rangle|^2$ represents the probability of sampling the kth target in the ansatz state. Therefore, the cost function $C_p(\boldsymbol{\theta}, \boldsymbol{\phi}) = 1 - \sum_{k=1}^{M} \Pr(k)$ represents the probability of failure to sample the target states, i.e., the probability of search failure.

The ansatz and transformation can be effectively viewed as two-dimensional states and SU(2) unitary operators, respectively. We define

$$|\bar{0}\rangle := \frac{1}{\sqrt{N-M}} \sum_{x \notin \boldsymbol{w}} |x\rangle, \quad |\bar{1}\rangle := \frac{1}{\sqrt{M}} \sum_{k=1}^{M} |w_k\rangle,$$

and $\beta := 2 \arcsin(\sqrt{M/N})$. The initial state can be rewritten as

$$|+\rangle^{\otimes n} = \cos\frac{\beta}{2}|\bar{0}\rangle + \sin\frac{\beta}{2}|\bar{1}\rangle. \tag{11}$$

Accordingly, in the two-dimensional subspace spanned by $\{|\bar{0}\rangle, |\bar{1}\rangle\}$, the action of the unitary at each QAOA layer $U(\theta_i, \phi_i)$ can be represented as a product of two rotations (up to a global phase), since

$$V(\theta_i, \phi_i) = e^{i(\theta_i + \phi_i)/2} R_n(\theta_i) R_z(\phi_i). \tag{12}$$

Here $R_n(\theta_i) := e^{-i\theta_i(\sin\beta\bar{X} + \cos\beta\bar{Z})/2}$ and $R_z(\phi_i) := e^{-i\phi_i\bar{Z}/2}$ with $\bar{X} := |\bar{0}\rangle\langle\bar{1}| + |\bar{1}\rangle\langle\bar{0}|$ and $\bar{Z} := |\bar{0}\rangle\langle\bar{0}| - |\bar{1}\rangle\langle\bar{1}|$. In this way, the problem is reduced to an optimization problem in a two-dimensional subspace spanned by $\{|\bar{0}\rangle, |\bar{1}\rangle\}$. For more details on the above content, see Refs. [16–18].

III. MAIN RESULTS

A. Critical problem hardness

In the context of a search problem with M marked items among a total of N items, the scale of multiple-target Grover search is $O(\sqrt{N/M})$ (see Ref. [22]). Consequently, the difficulty of variational Grover search exhibits a negative correlation with the solution density, defined as the fraction of marked items M/N. To quantify the difficulty of variational Grover search, we introduce the concept of problem hardness, defined as $\alpha := -\log_2(M/N)$, providing a measure of the reachability deficit.

The definition of problem hardness aims to capture the difficulty inherent in a search problem. When $M = 1$, α reduces to the metric in Ref. [19] for a single-target search problem.

As a function of problem hardness, the minimal cost function achievable by a depth-p QAOA circuit is defined as

$$C_p^*(\alpha) := \min_{(\boldsymbol{\theta}, \boldsymbol{\phi})} C_p(\boldsymbol{\theta}, \boldsymbol{\phi}, \alpha), \tag{13}$$

where the hardness-dependent cost function is

$$C_p(\boldsymbol{\theta}, \boldsymbol{\phi}, \alpha) := \langle \psi_p(\boldsymbol{\theta}, \boldsymbol{\phi}) | H_C | \psi_p(\boldsymbol{\theta}, \boldsymbol{\phi}) \rangle. \tag{14}$$

Here the dependence of the cost function on problem hardness α is implicit in both the cost Hamiltonian and the corresponding unitary operators V_C.

Next we give an analytical expression for the minimal cost function $C_p^*(\alpha)$.

Theorem 1. Given the problem hardness α and the depth p, the minimal cost function $C_p^*(\alpha)$ achievable by a depth-p QAOA circuit is given by

$$C_p^*(\alpha) = \cos^2\left[\min\left\{\frac{\pi}{2}, (2p+1)\arcsin(2^{-\alpha/2})\right\}\right]. \tag{15}$$

We give the proof in Appendix A. According to Theorem 1, when the number of targets decreases, the problem hardness α increases and so does the minimal cost function $C_p^*(\alpha)$. This implies that the search problem becomes more difficult for the QAOA when there are fewer targets, which is consistent with our intuition.

Here we would like to identify a critical problem hardness α_c so that the corresponding search problem can be solved perfectly even for depth-1 QAOA circuits. Formally, we have $C_1^*(\alpha) = 0$ if and only if $\alpha \leqslant \alpha_c$. Note that the definition above is valid for arbitrary qubit number n. Intuitively, when $\alpha \leqslant \alpha_c$, the number of marked items in the search problem is excessively large compared to the total number of items, which makes it easy to solve, even for a depth-1 QAOA. Moreover, we can also relax the definition to ε-approximate critical problem hardness. For $\varepsilon > 0$, define an ε-approximate critical problem hardness $\alpha_c(\varepsilon)$ such that when $\alpha \leqslant \alpha_c(\varepsilon)$, we have $C_1^*(\alpha) \leqslant \varepsilon$. Since the cost function represents the probability of search failure, this relaxation means that the algorithm allows a failure probability of no more than ε.

We would like to establish an analytical expression for α_c and $\alpha_c(\varepsilon)$. With the analytical expression of Eq. (15), we can obtain analytical expressions for the ε-approximate critical problem hardness $\alpha_c(\varepsilon)$.

Corollary 1 (critical problem hardness). In the variational Grover search, the ε-approximate critical problem hardness is

given by

$$\alpha_c(\varepsilon) = -\log_2\left[\sin^2\left(\tfrac{1}{3}\arccos\sqrt{\varepsilon}\right)\right]. \tag{16}$$

For $\varepsilon \ll 1$, we have $\arccos(\sqrt{\varepsilon}) = \pi/2 - \sqrt{\varepsilon} + O(\varepsilon^{3/2})$ and Eq. (16) can be represented in the asymptotic form

$$\alpha_c(\varepsilon) \approx -\log_2\left(\frac{1}{4} - \frac{\sqrt{\varepsilon}}{2\sqrt{3}}\right). \tag{17}$$

Correspondingly, the critical solution density M/N is

$$\frac{M}{N} \approx \frac{1}{4} - \frac{\sqrt{\varepsilon}}{2\sqrt{3}}. \tag{18}$$

When $\varepsilon = 0$, the critical problem hardness is $\alpha_c = 2$, corresponding to $M = N/4$. This implies that when $M \geqslant N/4$, perfect Grover search can be achieved with only a single depth. We note that this observation has been discussed in Ref. [21] for the multitarget Grover search.

B. Reachability deficit of variational Grover search

Here we analyze reachability deficit (RD) for variational Grover search. In Ref. [19], the reachability of a depth-p QAOA for a given problem is the difference between $C_p^*(\alpha)$ and the minimum eigenvalue of H_C. For search problems, the form of H_C has a minimum eigenvalue of 0. Therefore, the reachability of a depth-p QAOA ansatz solving the search problem is equal to $C_p^*(\alpha)$, which depends on the problem hardness α and depth p.

Recall that when the problem hardness $\alpha \leqslant \alpha_c$, the search problem can be solved perfectly by depth-1 QAOA circuits. So in this regime there will be no reachability deficit. With that, we formally define the reachability deficit below, which is adapted from Ref. [19].

Definition 1 (reachability deficit). For any search problem with problem hardness $\alpha > \alpha_c$, reachability deficit dictates that there is a critical depth $p^*(\alpha)$ for variational Grover search such that for $p < p^*(\alpha)$, we have $C_p^*(\alpha) > 0$.

Recall that $C_p^*(\alpha) > 0$ means that the QAOA circuit does not reach the global minimum, regardless of the classical optimization. Since the QAOA is an approximation algorithm, the exact solution is not achievable in most cases. Therefore, it is appropriate to extend the definition of RD to allow for a small failure probability ε.

Definition 2 (ε-approximate reachability deficit). Given an $\varepsilon > 0$, for any search problem with problem hardness $\alpha > \alpha_c(\varepsilon)$, ε-approximate reachability deficit dictates that there is a critical depth $p_\varepsilon^*(\alpha)$ for variational Grover search such that for $p < p_\varepsilon^*(\alpha)$, we have $C_p^*(\alpha) > \varepsilon$.

The critical depth in this definition can be obtained from Theorem 1 by solving $C_p^*(\alpha) = \varepsilon$ for p.

Corollary 2 (critical depth). In variational Grover search, for a fixed problem hardness α, the smallest circuit depth to achieve the minimal cost function $C_p^*(\alpha) \leqslant \varepsilon$ is given by

$$p_\varepsilon^*(\alpha) = \left\lceil \frac{\arccos\sqrt{\varepsilon}}{2\arcsin(2^{-\alpha/2})} - \frac{1}{2} \right\rceil. \tag{19}$$

When the failure probability $\varepsilon \ll 1$ and $\alpha \gg 1$, the critical depth asymptotically exhibits the form

$$p_\varepsilon^*(\alpha) \approx \left\lceil \frac{\pi - 2\sqrt{\epsilon}}{4}\sqrt{\frac{N}{M}} - \frac{1}{2} \right\rceil. \tag{20}$$

Note that if $\varepsilon = 0$ and $N \gg M$, we obtain the notable Grover search scale [22]

$$p^*(\alpha) \approx \left\lceil \frac{\pi}{4}\sqrt{\frac{N}{M}} - \frac{1}{2} \right\rceil. \tag{21}$$

In words, for a fixed large hardness, the critical depth decays linearly with the square root of the failure probability $\sqrt{\varepsilon}$ from the Grover search scale, when $\varepsilon \ll 1$. On the other hand, being similar to Eq. (18), we obtain the relation between a given depth p_ε^* and the solution density M/N:

$$\frac{M}{N} = \sin^2\left(\frac{\arccos\sqrt{\varepsilon}}{2p_\varepsilon^* + 1}\right). \tag{22}$$

We also construct the optimal search strategies reaching the minimal cost function $C_p^*(\alpha)$. We discuss one below and give others in Appendix B. First, one takes p QAOA blocks (or Grover iterates) with both angles set to π so that the state is close enough to the target state. Here "close enough" means that the target will be missed if another π rotation block is applied. Then the rotation angle for the last step is adjusted in order to reach $C_{p+1} = 0$. More specifically, the two angles in the last block are given by

$$\phi_{p+1} = \arccos\left\{-\cot\left[\left(p + \tfrac{1}{2}\right)\beta\right]\cot\beta\right\}, \tag{23}$$

$$\theta_{p+1} = 2\,\mathrm{arccot}(-\tan\phi_{p+1}\cos\beta), \tag{24}$$

where $\beta = 2\arcsin(2^{-\alpha/2})$. This parameter set was first obtained in Ref. [15]. Note that, according to Corollary 2, we have $p + 1 = p^*(\alpha)$ (see Appendix B for a detailed discussion).

The analytical results derived above represent an optimum performance that can be achieved. To further verify the practical feasibility and effectiveness of the variational optimization process, we numerically simulate the QAOA for the Grover search problem. We minimize the cost function by the BFGS optimizer provided by the PYTHON library SCIPY [24]. The numerical results for the critical depth $p_\varepsilon^*(\alpha)$ to reach $C_p \leqslant \varepsilon$ are shown in Fig. 1. The numerical results are close to the optimum performance that can be achieved. Moreover, the relation between C_p and the depth p is shown in Fig. 2(a) and the relation between C_p and the density α is shown in Fig. 2(b).

C. Case of the lower-order mixing Hamiltonian

The discussion above is based on the mixing Hamiltonian $H_B = (|+\rangle\langle+|)^{\otimes n}$, whose Pauli expansion is given by

$$H_B = \frac{1}{2^n}\left(\mathbb{I}^{\otimes n} + \sum_{l=1}^{n} P_l\right), \tag{25}$$

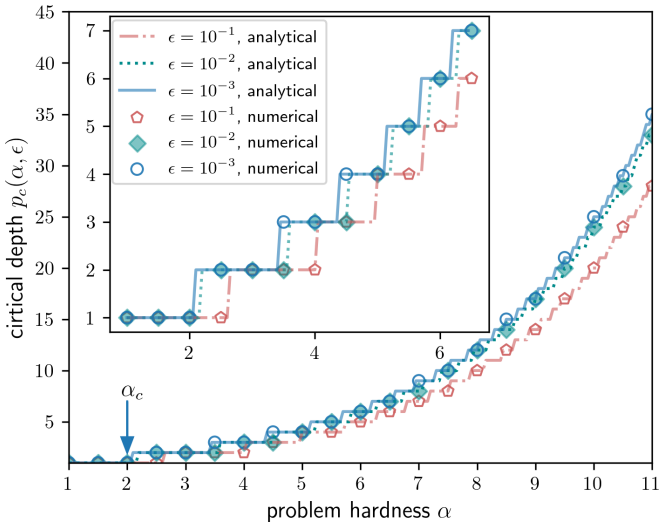

FIG. 1. Critical depth $p^*_\varepsilon(\alpha)$ versus the problem hardness α. Here ε is the required failure probability. The dash-dotted line, dotted line, and solid line represent the analytical results for ε values of 10^{-1}, 10^{-2}, and 10^{-3} respectively. The pentagons, diamonds, and circles correspond to the numerical results for the three required failure probabilities. The horizontal axis indicated by the arrow is the critical density α_c. The inset is a close-up of the main panel.

where

$$P_l = \sum_{i_1=1}^{n-l+1} \sum_{i_2>i_1}^{n-l+2} \cdots \sum_{i_l>i_{l-1}}^{n} X_{i_1} X_{i_2} \cdots X_{i_l}. \tag{26}$$

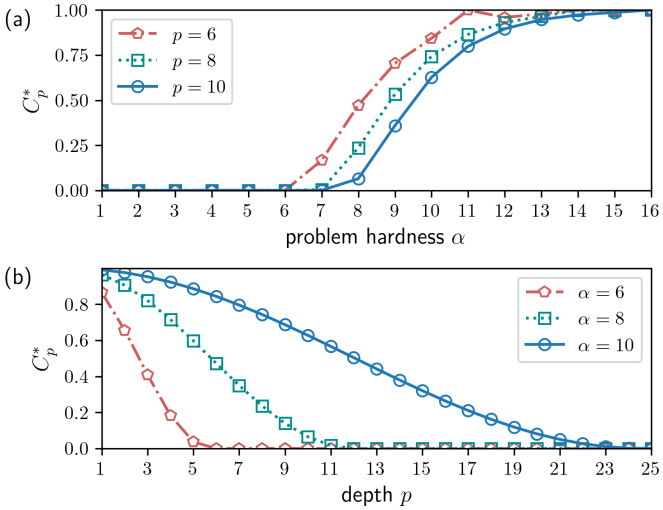

FIG. 2. Reachability deficit of variational Grover search. (a) Numerical simulation of the minimum cost function C^*_p versus problem hardness α. As the problem hardness increases, the minimum cost function monotonically increases. (b) Numerical simulation results of the minimum cost function C^*_p as a function of circuit depth p. The results show that as the depth increases, the minimum cost function monotonically decreases. In addition, for a given problem hardness, there exists a critical depth such that when the circuit depth exceeds the critical depth, the minimum cost function $C^*_p = 0$ can be achieved.

Here we have defined $X_i := \mathbb{I}^{\otimes i-1} \otimes \sigma_x \otimes \mathbb{I}^{\otimes n-i}$. The highest-order term $X_1 X_2 \cdots X_n$ includes the operation at all qubits, so H_B requires a many-body interaction with all qubits involved.

We define the qth-order mixing Hamiltonian as the cutoff of Eq. (25) up to the qth term (the zeroth-order term $\mathbb{I}$ is removed for the sake of simplicity)

$$H_B^{(q)} := \sum_{l=1}^{q} P_l. \tag{27}$$

Note that Eq. (27) reduces to Eq. (25) when $q = n$ (up to a factor $1/2^n$).

In Ref. [10], an algorithm employing a variational search approach was presented, utilizing the first-order mixing Hamiltonian $H_B^{(1)} = \sum_i X_i$. However, it should be noted that this method, as described in the literature, can ensure only a 50% probability of successfully locating the desired result. Consequently, it becomes intriguing to investigate the performance of lower-order mixing Hamiltonians and their potential to achieve flawless search outcomes through the utilization of an optimizer. To address this question comprehensively, we conducted a numerical analysis of the reachability deficit associated with variational Grover searches employing low-order mixing Hamiltonians. The specific details of the numerical method employed for this investigation are outlined in Appendix C.

In Fig. 3(a) we present numerical simulations investigating the performance of first-order and second-order approximate mixing Hamiltonians in a single target search with $n = 6$ qubits. The simulations entail optimizing the results based on various initial guesses. A comparison is made with the case where the mixing Hamiltonian is $H_B = (|+\rangle\langle+|)^{\otimes n}$. For different mixing Hamiltonians, we use a fixed cost Hamiltonian H_C (see Appendix C). Our findings consistently demonstrate that H_B achieves the first C^*_p value for all QAOA depths p. Furthermore, as the order q increases, the values obtained for different q converge towards the value achieved by H_B. Notably, the second-order approximation already exhibits a comparable performance to H_B, and even with a first-order mixing Hamiltonian, we achieve perfect search outcomes.

We further conduct simulations to examine the relationship between the critical depth $p^*(\alpha)$ and the problem hardness α while considering different mixing Hamiltonians. The simulation involves a system of 12 qubits, as illustrated in Fig. 3(b). The figure depicts the shaded area, with the upper and lower edges determined by

$$p_{\text{up}}(\alpha) = \frac{7\pi}{24 \arcsin(2^{-\alpha/2})} + 2, \tag{28}$$

$$p_{\text{low}}(\alpha) = \frac{\pi}{4 \arcsin(2^{-\alpha/2})} - \frac{1}{2}, \tag{29}$$

respectively. It is worth noting that as the problem hardness increases, the behavior of the first-order approximate mixer gradually approaches the upper edges of the shaded region. Consequently, we can ascertain its critical depth numerically, considering it to be approximated by p_{up} as defined in Eq. (28). This indicates that even for a first-order approximation, the critical depth required to achieve perfect variational

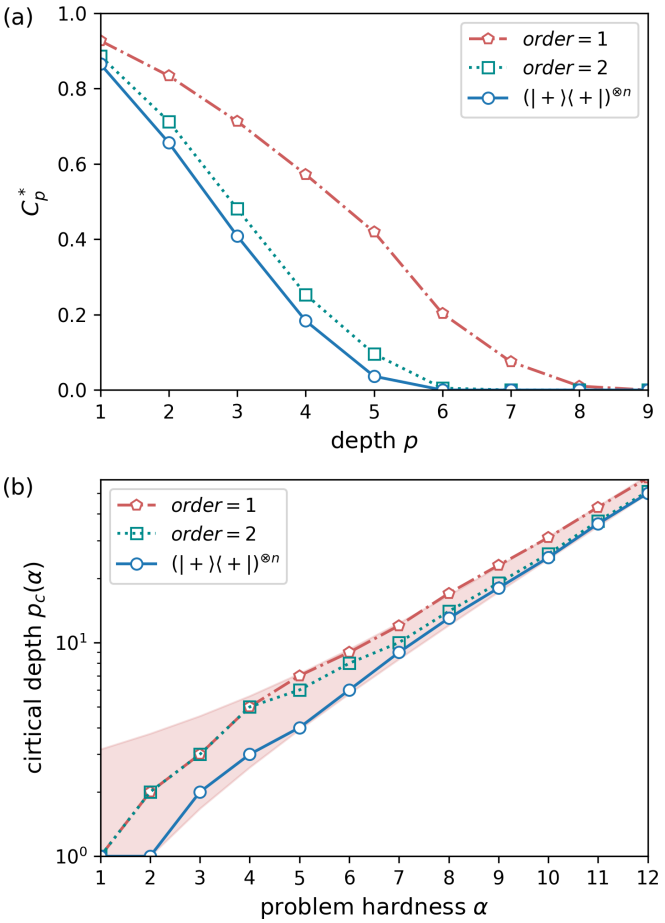

FIG. 3. Numerical simulation of the reachability deficit for the first-order and second-order approximate mixing Hamiltonian. (a) Minimum cost function C_p^* versus circuit depth p. (b) Critical depth $p^*(\alpha)$ vs problem hardness α. The blue solid line represents the case where the mixing Hamiltonian is $H_B = (|+\rangle\langle+|)^{\otimes n}$ and the red dash-dotted and green dotted lines represent the cases of first-order and second-order approximate mixing Hamiltonians, respectively. We simulate a six-qubit system with a problem hardness $\alpha = 6$ in (a). The results show that a higher-order approximate mixing Hamiltonian may have better performance, with H_B having the best performance. The upper and lower edges of the shaded area in (b) are given by expressions of p_{up} and p_{low} in Eqs. (28) and (29), respectively. Note that the first-order approximation asymptotically conforms to the upper boundary numerically, while the second-order approximation approaches the behavior in the case of H_B.

Grover search is $O(2^{\alpha/2})$, i.e., $O(\sqrt{N/M})$. In addition, the asymptotic behavior of the second-order approximate mixing Hamiltonian approaches that of H_B.

Hence, in scenarios where the practical implementation of nonlocal interactions proves challenging, employing a lower-order approximation of H_B can be a viable alternative, with the expectation of achieving comparable performance. This insight indicates that using a more localized mixed Hamiltonian as a feasible alternative to projection operators has great potential, especially in the mitigation of constraints of the NISQ era.

IV. CONCLUSION

This study delved into the reachability deficit problem in variational Grover search, with the failure probability of finding targets as the cost function. We introduced the notion of problem hardness as a convenient metric for quantifying problem complexity, which is a rescaling of the solution density and is compatible with the single-target search scenario presented in Ref. [19].

In our investigation of multitarget search scenarios, we analytically computed the minimum cost function for any circuit depth. We established a critical problem hardness that determines the feasibility of meeting a given failure probability requirement in a single-depth variational quantum search. If the problem hardness falls below this critical value, a single layer of the QAOA is sufficient to meet the failure probability requirement. For zero failure probability tolerance, we identified the problem hardness corresponding to a perfect search, defined as $\alpha_c = 2$, which aligns with prior research [21]. Furthermore, we derived an expression for the critical depth that ensures satisfying the failure probability requirement for a given problem hardness. Whenever the circuit depth is greater than or equal to the critical depth, the search fulfilling the failure probability requirement can be achieved. To validate our analytical results, we conducted variational optimization simulations, which closely matched the analytical predictions, confirming their achievable. However, the analysis method employed in this paper exclusively pertains to the variational Grover search. Applying our methodology to more complex QAOA applications is left for future exploration.

To explore deeper into the reachability deficit problem, we conducted numerical simulations employing low-order Pauli approximations of the projective operator as the mixing Hamiltonian. The results underscore the detrimental impact of a contracted mixing Hamiltonian on the reachability deficit. Nevertheless, within the simulation range of problem hardness, we observed that the critical depth for the first-order approximation scaling is $O(\sqrt{N/M})$. Additionally, the second-order approximation asymptotically approaches the performance level of the projective operator with increasing problem hardness. This insight suggests the promising potential of utilizing more localized mixing Hamiltonians as viable alternatives to projective operators, especially in the context of the NISQ era.

In summary, our research advances the understanding of the reachability deficit problem in variational Grover search, offering valuable insights into optimizing search performance and exploring alternative mixing Hamiltonians. These findings contribute to the development and applicability of variational quantum algorithms in practical quantum computing scenarios.

ACKNOWLEDGMENTS

This work was supported by the National Natural Science Foundation of China (Grants No. 11875160 and No. U1801661), the Natural Science Foundation of Guangdong Province (Grant No. 2017B030308003), the Science, Technology and Innovation Commission of Shenzhen Municipality (Grants No. JCYJ20170412152620376,

No. JCYJ20170817105046702, and No. KYTDPT20181011104202253), the Key R&D Program of Guangdong province (Grant No. 2018B030326001), the Economy, Trade and Information Commission of Shenzhen Municipality (Grant No. 201901161512), and Guangdong Provincial Key Laboratory (Grant No. 2019B121203002). We gratefully acknowledge Kaiming Bian for his insightful discussions of this research.

APPENDIX A: PROOF OF THEOREM 1

Lemma 1. Letting $\gamma_i := 2\arcsin(\sin\beta\sin\frac{\theta_i}{2})$ and $\Gamma := 2\text{acos}\sqrt{C_p} - \beta$, we have

$$|\Gamma| \leqslant \sum_{i=1}^{p} |\gamma_i|. \tag{A1}$$

Proof. Because $C_p = 1 - |\langle\bar{1}|\psi_p(\theta,\phi)\rangle|^2 = 1 - |\langle\bar{1}|U_p(\theta,\phi)|+\rangle^{\otimes n}|^2$, a unitary $U_p(\theta,\phi)$ approaching the cost function C_p can always be written as

$$U_p(\theta,\phi) = R_z(*)R_y(\Gamma')R_z(*), \tag{A2}$$

where the y-rotation angle $|\Gamma'| \geqslant |\Gamma|$ and the asterisk denotes arbitrary angle values.

We perform z-y-z decomposition on $R_n(\theta_i)R_z(\phi_i)$, which gives $R_n(\theta_i)R_z(\phi_i) = R_z(*)R_y(\gamma_i)R_z(*)$, where $\gamma_i = 2\arcsin(\sin\beta\sin\frac{\theta_i}{2})$. We further define $\gamma_{1:q} \in [-\pi,\pi]$ as the angle satisfying

$$\sum_{i=1}^{q} R_n(\theta_i)R_z(\phi_i) = R_z(*)R_y(\gamma_{1:q})R_z(*). \tag{A3}$$

Note that $\gamma_{1:1} = \gamma_1$ and $\Gamma' = \gamma_{1:p}$. In the following, we show by induction that when $|\gamma_{1:q}| \in [0,\pi]$,

$$|\gamma_{1:q}| \leqslant \sum_{i=1}^{q} |\gamma_i| \tag{A4}$$

is satisfied for all $q \in [1,p]$.

When $q = 1$, Eq. (A4) is trivially satisfied. When $q > 1$, we have $\sum_{i=1}^{q-1} R_n(\theta_i)R_z(\phi_i) = R_z(*)R_y(\gamma_{1:q-1})R_z(*)$. Therefore, $R_n(\theta_p)R_z(\phi_q)\sum_{i=1}^{q-1} R_n(\theta_i)R_z(\phi) = R_z(*)R_y(\gamma_q)R_z(*)R_y(\gamma_{1:q-1})R_z(*) = R_z(*)R_y(\gamma_{1:q})R_z(*)$, or equivalently

$$R_y(\gamma_q)R_z(*)R_y(\gamma_{1:q-1}) = R_y(\gamma_{1:q}). \tag{A5}$$

After performing the expansion $R_z(\alpha) = \cos(\alpha/2)\mathbb{I} - i\sin(\alpha/2)\sigma_z$ and $R_y(\alpha) = \cos(\alpha/2)\mathbb{I} - i\sin(\alpha/2)\sigma_y$ for each element in Eq. (A5), we can find the relation $\cos^2(*)\sin^2[(\gamma_q + \gamma_{1:q-1})/2] = \sin^2(\gamma_{1:q}/2)$. So we have $\sin^2[(\gamma_q + \gamma_{1:q-1})/2] \geqslant \sin^2(\gamma_{1:q}/2)$. Therefore, when $|\gamma_{1:q}| \in [0,\pi]$, we have $|\gamma_{1:q}| \leqslant |\gamma_{1:q-1}| + |\gamma_q|$. We can immediately obtain $|\gamma_{1:q}| \leqslant \sum_{i=1}^{q} |\gamma_i|$ by mathematical induction.

So Eq. (A4) is satisfied for all q. Because $|\Gamma| \leqslant |\Gamma'| = |\gamma_{1:p}|$, Lemma 1 holds true. ■

Based on Lemma 1, the proof of Theorem 1 is as follows.

Proof. According to Lemma 1 and noting that $\gamma_i \in [-2\beta, 2\beta]$, we obtain $|2\beta p| \geqslant |\Gamma| = 2\text{acos}\sqrt{C_p} - \beta$. When $|(2p+1)\arcsin(2^{-\alpha/2})| \leqslant \pi/2$ we have $C_p \geqslant \cos^2[(2p+1)\arcsin(2^{-\alpha/2})]$. Therefore, $C_p \geqslant C_p^*$ is necessary.

Then we just need to construct a searching parameter set with $C_p = C_p^*$. Actually, Ref. [15] has shown that the perfect quantum search can be realized by a set of π rotations plus an adjustment step. More specifically, C_p^* can be reached with the parameter set

$$\phi_i = \begin{cases} \pi, & i < p^* \\ \arccos\{-\cot[(p^* - \frac{1}{2})\beta]\cot\beta\}, & i = p^* \\ 0, & i > p^*, \end{cases}$$
$$\theta_i = \begin{cases} \pi, & i < p^* \\ 2\text{arccot}(-\tan\phi_i\cos\beta), & i = p^* \\ 0, & i > p^*, \end{cases} \tag{A6}$$

where $\beta = 2\arcsin(2^{-\alpha/2})$. In this way C_p^* can be reached with above parameter set, so Theorem 1 holds true. ■

APPENDIX B: OPTIMAL STRATEGIES FOR GROVER SEARCH

Theorem 1 gives a fundamental upper bound of achievable $p^*(\alpha)$. On the other hand, the protocols saturating the upper bound is not unique. Here we introduce three distinct schemes, each capable of attaining the target state with a probability of 1 when the depth $p = p^*(\alpha)$.

1. Phase-matching Grover search

The first scheme is phase-matching Grover search, which was first proposed by Long *et al.* [17]. Consider a constraint $\phi_1 = \phi_2 = \cdots = \phi_p := \phi$ and $\theta_1 = \theta_2 = \cdots = \theta_p := \theta$, which means that $U_p(\boldsymbol{\theta},\boldsymbol{\phi})$ defined in Eq. (7) is equivalent to a rotation in the Bloch sphere,

$$U_p(\boldsymbol{\theta},\boldsymbol{\phi}) = R_m(p\alpha), \tag{B1}$$

where the rotation $R_m(\cdot)$ and angle α are defined by

$$R_m(\alpha) := R_n(\theta)R_z(\phi). \tag{B2}$$

We denote the axis of this rotation by $\boldsymbol{m}$. The necessary condition of optimal search is that $\boldsymbol{m}$ must be perpendicular to the Bloch vector of both states $|+\rangle^{\otimes n}$ and $|\bar{1}\rangle$, since the trajectory must pass through the start and end points. This condition is just the phase-match condition, which requires $\phi = -\theta$. Based on this constraint, we can solve the optimal parameter setting by a geometric method; the result is

$$\phi = -\theta = \pm 2\arcsin\left(\frac{\sin(\frac{\pi}{4p+2})}{\sin(\beta/2)}\right). \tag{B3}$$

Since $\sin[\pi/(4p+2)]/\sin(\beta/2) \leqslant 1$, we can immediately check that this parameter setting requires that $p \geqslant p^*(\alpha)$. The trajectories of the states in this scheme on the Bloch sphere are shown in Fig. 4(a).

2. Brassard's algorithm

The second scheme has been given in main text. Here we explain why $p + 1 = p^*(\alpha)$. Based on the fact that $\langle\bar{0}|\bar{1}\rangle = 0$, we can solve the parameters of the last step (θ,ϕ) through the

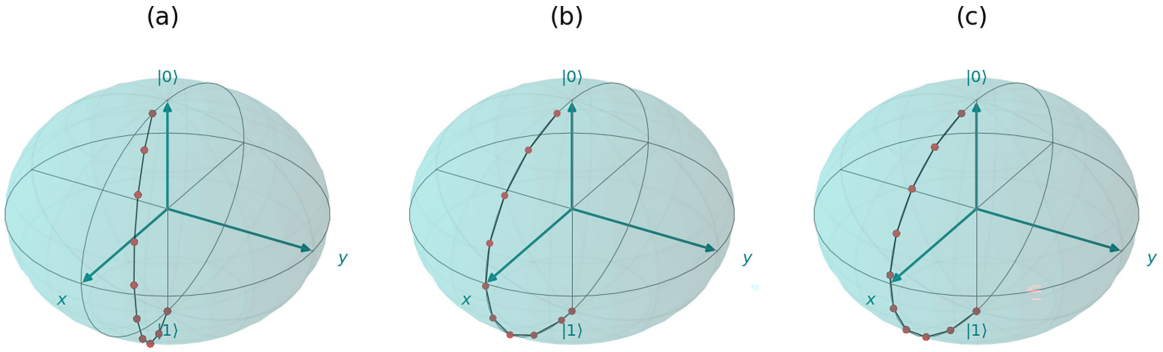

FIG. 4. Trajectory of the states in each depth for different optimal algorithms. (a) Phase-matching Grover search (Long's algorithm), In this scheme, the trajectory of the quantum state does not lie on the geodesic of the Bloch sphere, but the arc length for each step is uniform. (b) Brassard's algorithm, whose parameter setting is given in the main text. In this scheme, the trajectory lies on the geodesic of the Bloch sphere. For the first $p-1$ steps, the arc length for each step is 2β, while the arc length for the final step is determined by $\pi-(2p+1)\beta$ to ensure that the final trajectory lands on the south pole of the Bloch sphere. (c) Equal interval geodesic scheme. In this scheme, the trajectory lies on the geodesic of the Bloch sphere and the arc length for each step is $(\pi-\beta)/p$.

equation [15]

$$\langle\bar{0}|R_n(\theta)R_z(\phi)[R_n(\pi)R_z(\pi)]^p|+\rangle^{\otimes n}=0. \tag{B4}$$

In Eq. (23), since the domain of definition of $\arccos(x)$ is $[-1,1]$, we must have

$$\left|\cot\left[\left(p+\tfrac{1}{2}\right)\beta\right]\cot\beta\right|\leqslant 1. \tag{B5}$$

Note that $(p+\frac{1}{2})\beta$ is close to $\pi/2$ and we have $\pi/2\beta-\frac{3}{2}\leqslant p\leqslant\pi/2\beta-\frac{1}{2}$. Thus, the depth p that satisfies the requirement is given by

$$p=\left\lceil\frac{\pi}{2\beta}-\frac{3}{2}\right\rceil, \tag{B6}$$

and hence we have $p+1=p^*(\alpha)$ when we set $\beta=2\arcsin(2^{-\alpha/2})$. The trajectories of the states in this scheme on the Bloch sphere are shown in Fig. 4(b).

3. Equal interval geodesic scheme

Finally, we introduce a scheme known as the equal interval geodesic scheme. This scheme assumes that the trajectory of each step follows a geodesic curve, with an equal variation of the polar angle. For the state $|\psi_m\rangle=\cos\frac{\beta_m}{2}|\bar{0}\rangle+\sin\frac{\beta_m}{2}|\bar{1}\rangle$, where $\beta_0:=\beta$ and $\beta_m:=m(\pi-\beta)/p$ $(m>0)$, we solve the equation $|\psi_m\rangle=R_n(\theta_m)R_z(\phi_m)|\psi_{m-1}\rangle$ to obtain the expressions

$$\phi_m=\arccos\left(\frac{\sin\beta_m+\cot\beta(\cos\beta_m-\cos\beta_{m-1})}{\sin\beta_{m-1}}\right),$$

$$\theta_m=\arccos\times\left(\frac{\sin\beta_{m-1}\cos\phi_m\cos\beta-\sin\beta\cos\beta_{m-1}}{\sqrt{1-(\sin\beta_{m-1}\sin\beta\cos\phi_m+\cos\beta\cos\beta_{m-1})^2}}\right). \tag{B7}$$

This scheme offers a systematic approach to determine the values of ϕ_m and θ_m, providing a structured trajectory for the quantum states. In Fig. 4(c) we depict the trajectories of the states in this scheme on the Bloch sphere.

Since the domain of the arccos function is $[-1,1]$, according to the first of Eqs. (B7), we have the inequality

$$-1\leqslant\frac{\sin\beta_m+\cot\beta(\cos\beta_m-\cos\beta_{m-1})}{\sin\beta_{m-1}}\leqslant 1. \tag{B8}$$

This leads to $\beta_{m-1}\leqslant\beta_m\leqslant\beta_{m-1}+2\beta$. By the definition of β_m, we immediately have

$$p\geqslant\frac{\pi}{2\beta}-\frac{1}{2}. \tag{B9}$$

This is consistent with the expression for the critical depth $p^*(\alpha)$ as presented in Eq. (21), since when $p\geqslant p^*(\alpha)$, a perfect search can be achieved.

APPENDIX C: DETAILS OF NUMERICAL SIMULATION

For simplicity, we set the target items to the last M items. In this way, H_C has the form

$$H_C=\begin{bmatrix}1&&&&\\&1&&&\\&&\ddots&&\\&&&0&\\&&&&0\end{bmatrix}. \tag{C1}$$

Thus, the unitary operator $V_C(\phi)$ is given by

$$V_C(\phi)=\begin{bmatrix}1&&&&\\&1&&&\\&&\ddots&&\\&&&e^{i\phi}&\\&&&&e^{i\phi}\end{bmatrix}. \tag{C2}$$

Considering α is an integer, we then have that $m=\log_2 M=n-\alpha$ is also an integer. Thus, the unitary operator for integer m can be constructed as the quantum gate shown in Fig. 5(a). Here we use the phase shift gate

$$\mathrm{PS}(\phi)=\begin{bmatrix}1&0\\0&e^{i\phi}\end{bmatrix}. \tag{C3}$$

In fact, the quantum gate in Fig. 5(a) means that if all of the control qubits and the target qubit are in $|1\rangle$, the corresponding states obtain a phase $e^{i\phi}$, regardless of the value of the

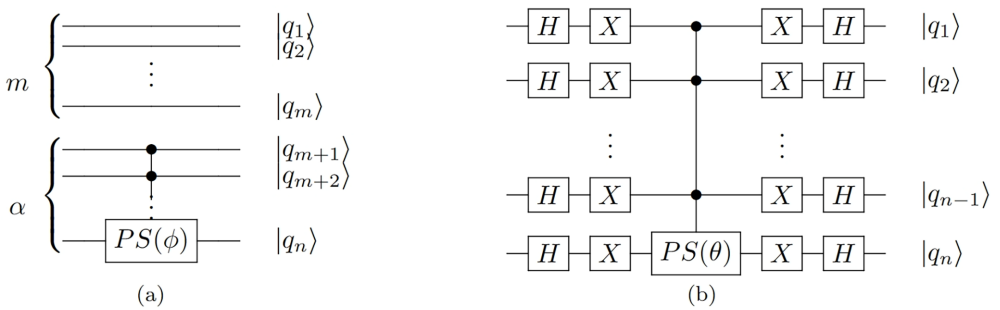

FIG. 5. Construction of unitary operators (a) $V_C(\phi)$ and (b) $V_B(\theta)$. (a) $V_C(\phi) = (\mathbb{I}_{2^n-2^m}) \oplus (e^{i\phi}\mathbb{I}_{2^m})$. The first m qubits remain idle, while the subsequent α qubits are subjected to a controlled phase shift gate. (b) $V_B(\theta) = H^{\otimes n}(e^{i\theta} \oplus \mathbb{I}_{2^n-1})H^{\otimes n}$. For details see Refs. [11,25].

idle qubits. For the case when the target items are located at other positions, the corresponding $V_C(\phi)$ can be constructed by adjusting the positions of idle qubits and applying some X unitary transformations.

Since $(|+\rangle\langle+|)^{\otimes n} = H^{\otimes n}(|0\rangle\langle 0|)^{\otimes n}H^{\otimes n}$ and $V_B(\theta) = \mathbb{I} - (1 - e^{i\theta})(|+\rangle\langle+|)^{\otimes n}$, the circuit of the unitary operator $V_B(\theta)$ can be constructed as in Fig. 5(b). For more details, refer to Refs. [11,25].

We have utilized the PYTHON library MINDQUANTUM [26] to simulate the quantum circuits of variational Grover search, as well as the versions with lower-order approximation mixing Hamiltonians. In the classical optimization part, we utilized the BFGS and SLSQP optimizers from the PYTHON library SCIPY [24]. For the versions involving low-order approximation mixing Hamiltonians, the following scheme was employed for selecting initial parameters.

(i) For a single layer of the QAOA, we randomly initialize the parameters and repeat the optimization process 30 times. We select the instance with the first cost function value and store its corresponding optimal parameters in $(\boldsymbol{\theta}^{*(1)}, \boldsymbol{\phi}^{*(1)})$.

(ii) For multiple layers of the QAOA, the initial parameters are determined by the optimal parameters of the previous layer. Specifically, we set the initial guesses as

$$\boldsymbol{\theta}^{(p)} = \boldsymbol{\theta}^{*(p-1)} \oplus \theta_{p-1}^{*(p-1)}, \tag{C4}$$

$$\boldsymbol{\phi}^{(p)} = \boldsymbol{\phi}^{*(p-1)} \oplus \phi_{p-1}^{*(p-1)}. \tag{C5}$$

Here $\boldsymbol{\theta}^{(p)} = [\theta_1^{(p)}, \ldots, \theta_p^{(p)}]$ and $\boldsymbol{\phi}^{(p)} = [\phi_1^{(p)}, \ldots, \phi_p^{(p)}]$ are the parameters of the p-depth QAOA ansatz.

This initialization scheme is inspired by the work presented in Ref. [27]. It demonstrates good optimization performance for first-order and second-order versions. However, higher-order approximation mixing Hamiltonians encounter significant challenges in escaping local minima. Additionally, as the order q increases, the number of multiqubit gates grows polynomially with respect to qubit number n in $V_B(\theta)$, making circuit simulation more difficult.

[1] E. Farhi, J. Goldstone, and S. Gutmann, A quantum approximate optimization algorithm, arXiv:1411.4028.

[2] J. Choi and J. Kim, in *Proceedings of the Tenth International Conference on Information and Communication Technology Convergence, Jeju Island, 2019* (IEEE, Piscataway, NJ, 2019), pp. 138–142.

[3] M. Streif, S. Yarkoni, A. Skolik, F. Neukart, and M. Leib, Beating classical heuristics for the binary paint shop problem with the quantum approximate optimization algorithm, Phys. Rev. A **104**, 012403 (2021).

[4] A. Borle, V. Elfving, and S. J. Lomonaco, Quantum approximate optimization for hard problems in linear algebra, SciPost Phys. Core **4**, 031 (2021).

[5] E. Farhi, J. Goldstone, and S. Gutmann, A quantum approximate optimization algorithm applied to a bounded occurrence constraint problem, arXiv:1412.6062.

[6] J. S. Baker and S. K. Radha, Wasserstein solution quality and the quantum approximate optimization algorithm: A portfolio optimization case study, arXiv:2202.06782.

[7] P. Vikstål, M. Grönkvist, M. Svensson, M. Andersson, G. Johansson, and G. Ferrini, Applying the quantum approximate optimization algorithm to the tail-assignment problem, Phys. Rev. Appl. **14**, 034009 (2020).

[8] H. Mustafa, S. N. Morapakula, P. Jain, and S. Ganguly, in *Proceedings of the International Conference on Trends in Quantum Computing and Emerging Business Technologies, Pune, 2022* (IEEE, Piscataway, NJ, 2022), pp. 1–8.

[9] J. Choi, S. Oh, and J. Kim, Quantum approximation for wireless scheduling, Appl. Sci. **10**, 7116 (2020).

[10] Z. Jiang, E. G. Rieffel, and Z. Wang, Near-optimal quantum circuit for Grover unstructured search using a transverse field, Phys. Rev. A **95**, 062317 (2017).

[11] M. E. S. Morales, T. Tlyachev, and J. Biamonte, Variational learning of Grover quantum search algorithm, Phys. Rev. A **98**, 062333 (2018).

[12] D. An and L. Lin, Quantum linear system solver based on time-optimal adiabatic quantum computing and quantum approximate optimization algorithm, ACM Trans. Quantum Comput. **3**, 5 (2022).

[13] L. K. Grover, Quantum mechanics helps in searching for a needle in a haystack, Phys. Rev. Lett. **79**, 325 (1997).

[14] M. Boyer, G. Brassard, P. Høyer, and A. Tapp, Tight bounds on quantum searching, Fortschr. Phys. **46**, 493 (1998).

[15] G. Brassard, P. Høyer, M. Mosca, and A. Tapp, Quantum amplitude amplification and estimation, Contemp. Math. **305**, 53 (2002).

[16] G. L. Long, Grover algorithm with zero theoretical failure rate, Phys. Rev. A **64**, 022307 (2001).

[17] G. L. Long, X. Li, and Y. Sun, Phase matching condition for quantum search with a generalized initial state, Phys. Lett. A **294**, 143 (2002).

[18] J.-Y. Hsieh and C.-M. Li, A General SU(2) formulation for quantum searching with certainty, Phys. Rev. A **65**, 052322 (2002).

[19] V. Akshay, H. Philathong, M. E. S. Morales, and J. D. Biamonte, Reachability deficits in quantum approximate optimization, Phys. Rev. Lett. **124**, 090504 (2020).

[20] V. Akshay, H. Philathong, I. Zacharov, and J. Biamonte, Reachability deficits in quantum approximate optimization of graph problems, Quantum **5**, 532 (2021).

[21] D.-P. Chi and J. Kim, in *Proceedings of the First NASA International Conference on Quantum Computing and Quantum Communications, Palm Springs, 1998*, edited by C. P. Williams, Lecture Notes in Computer Science Vol. 1509 (Springer, Berlin, 1999), pp. 148–151.

[22] M. A. Nielsen and I. L. Chuang, *Quantum Computation and Quantum Information*, 10th Anniversary ed. (Cambridge University Press, Cambridge, 2010).

[23] E. Biham, O. Biham, D. Biron, M. Grassl, D. A. Lidar, and D. Shapira, Analysis of generalized grover quantum search algorithms using recursion equations, Phys. Rev. A **63**, 012310 (2000).

[24] P. Virtanen, R. Gommers, T. E. Oliphant, M. Haberland, T. Reddy, D. Cournapeau, E. Burovski, P. Peterson, W. Weckesser, J. Bright, S. J. van der Walt, M. Brett, J. Wilson, K. J. Millman, N. Mayorov, A. R. J. Nelson, E. Jones, R. Kern, E. Larson, C. J. Carey *et al.*, SciPy 1.0: Fundamental algorithms for scientific computing in Python, Nat. Methods **17**, 261 (2020).

[25] C. Figgatt, D. Maslov, K. A. Landsman, N. M. Linke, S. Debnath, and C. Monroe, Complete 3-qubit Grover search on a programmable quantum computer, Nat. Commun. **8**, 1918 (2017).

[26] MindQuantum, version 0.6.0, https://gitee.com/mindspore/mindquantum (2021).

[27] L. Zhou, S.-T. Wang, S. Choi, H. Pichler, and M. D. Lukin, Quantum approximate optimization algorithm: Performance, mechanism, and implementation on near-term devices, Phys. Rev. X **10**, 021067 (2020).